

AUTOMATIC BRAIN METASTASES PLANNING

Clinical White Paper

Radiosurgery has become the first-line treatment option for patients with multiple brain metastases, prolonging overall survival for younger patients when salvage treatment options are readily available¹. Treatment decisions are no longer based on the number of metastases but rather on the cumulative tumor volume², with hypo-fractionated radiosurgery regimens a viable alternative for patients with large disease burden³⁻⁶. Traditional radiosurgery approaches target each metastasis individually; prioritizing superior dose gradients over treatment efficiency as the total treatment time scales linearly with the number of metastases. Brainlab Automatic Brain Metastases Planning advances the radiosurgery legacy by targeting up to ten metastases at once; optimizing treatments both in terms of plan quality and delivery efficiency.

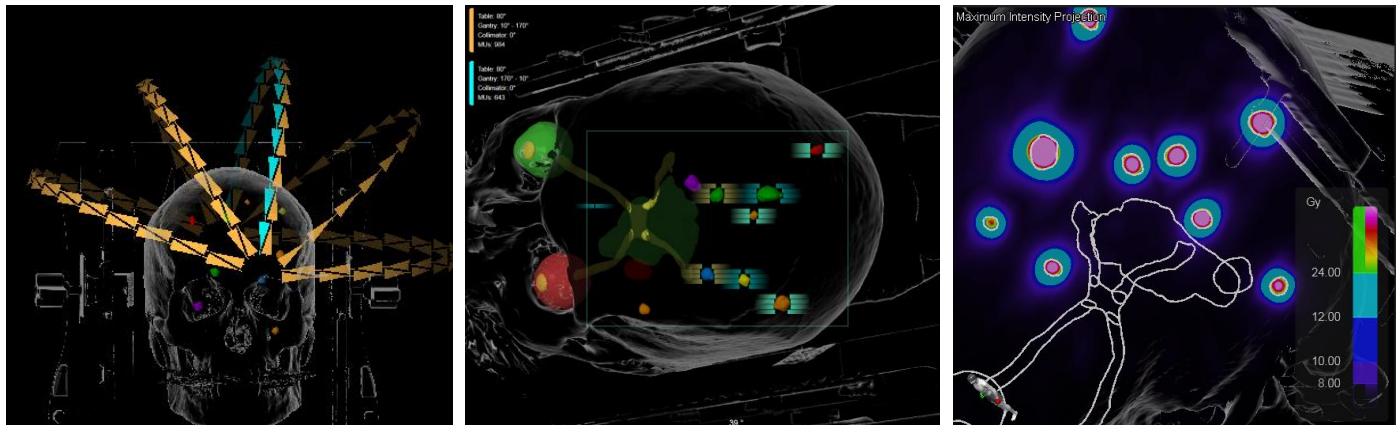


Figure 1: Automatic Brain Metastases Planning details for Patient 4 with 9 lesions.

The Assuta Medical Center located just north of Tel Aviv, along the popular Mediterranean coastline of Israel, has been a radiosurgery center of excellence for many years. Equipped with Novalis Radiosurgery and a high definition large field multi-leaf collimator, this center has been pioneering the clinical implementation of Brainlab Automatic Brain Metastases Treatment Planning. Starting treatments in summer 2014, they retrospectively selected ten early cases treated at their institution for review of the entire treatment planning and delivery process.

The detailed characteristics of the selected patient population can be found in Table 1. Ten patients over fifty years of age were selected with two to nineteen brain metastases; seven related to a primary lung cancer, two associated with breast cancer and one resulting from melanoma. The total accumulated treated volumes range from 0.15 cc to 19.78 cc. All lesions were identified on 1 mm T1 contrast-enhanced magnetic resonance imaging slices rigidly fused to 0.6 mm computed tomography slices.

Treatment planning starts with importing all DICOM data into the Elements treatment planning platform, fusing the various data sets and contouring the gross tumor volumes of each target on the magnetic resonance data sets utilizing the Smartbrush Element. All critical organs are automatically segmented based on a universal atlas approach and can be consulted in a dedicated DICOM Viewer.

Automatic Brain Metastases Planning takes the target volumes and models the patient outer contour and underlying table top for correct dose calculations. A list of numerous treatment templates matching diverse hospital practices can be defined upfront with the most appropriate template chosen for each patient. Treatment templates contain various information: possible enlargement of the tumor volumes to encompass biological and treatment uncertainties, different prescription doses in function of individual tumor volumes or sizes, table and gantry angle preferences as a guide for the subsequent automatic optimization of the arcs.

Table 1: Patient Characteristics

Patient Characteristics	Patient 1	Patient 2	Patient 3	Patient 4	Patient 5	Patient 6	Patient 7	Patient 8	Patient 9	Patient 10
Age at treatment	51	76	55	46	55	61	65	68	63	58
Gender	Female	Female	Female	Male	Female	Female	Male	Male	Female	Male
Neurological status	No deficit	Moderate Impairment	Some deficit	No deficit	Moderate Impairment	Some deficit	No deficit	No deficit	No deficit	Some deficit
Number of brain metastases	2	5	7	9	10	9	8	3	4	6
Volume of largest lesion treated (cc)	0.131	0.308	2.101	4.99	2.29	0.489	7.177	2.389	3.645	12.328
Total volume of metastases (cc)	0.151	1.046	4.774	9.451	4.091	2.007	14.904	3.563	6.378	19.782
Primary tumor localization	Lung	Breast	Lung	Melanoma	Lung	Lung	Lung	Lung	Breast	Lung

Automatic Brain Metastases Planning determines the isocenter position as the average position of the centers of mass of each individual target. The software uses the pre-defined table and gantry angles to create a set of two independent arcs per table angle. Depending on the hemisphere where the isocenter is located, the arcs are mirrored around the sagittal plane. The start and stop angles of the arc are first set to the template values and automatically modified during optimization. The leaf positions are shaped to conform the targets, with an additional margin of up to one millimeter—in addition to any margin that may have been defined in the template—for all fields of each arc.

To prevent irradiation of normal tissue, all targets must be assigned to specific arcs and not necessarily treated by all arcs at the same time. In the latter scenario, multiple targets may line up along the direction of motion of a leaf pair, which would cause the pair to open wide and also expose the healthy tissue between the targets. Therefore, each leaf pair is only allowed to expose one target at any time. For the sake of efficiency, the algorithm bases this choice on the principle that as many targets as possible should be treated by each arc. The choices are made so that the Monitor Units applied by all arcs are minimized.

Additionally, the collimator is rotated as much as possible to distribute the dosage spillage caused by radiation leakage between adjacent leaves. Although this rotation is limited because all targets treated by an arc still have to fit into the effective multi-leaf collimator field, its contribution to the protection of healthy tissue is still deemed to be significant.

After assigning individual targets to arcs, the weights of the arcs are optimized in terms of conformity and expressed by the inverse Paddick conformity index⁷, one for each target. During optimization, the region of normal tissue around each target for calculation of the conformity is limited to a margin of five millimeters.

In addition to optimizing the arc weights, the algorithm evaluates several other approaches to improve the conformity further, like adding or subtracting small margins around the targets with suboptimal conformity and varying start and stop angles of each arc. Details of a typical treatment plan are shown in Figure 1.

The entire treatment plan optimization typically can be performed in less than two minutes, after which the plan can be assessed in detail in dedicated views. An overview of the treatment plan characteristics for all ten patients can be found in Table 2.

All patients were treated with Novalis frameless radiosurgery technology. A unique triple layer thermoplastic mask is molded to each patient’s specific anatomy. The rigidity of this mask system is well-established with patients reportedly moving beyond one millimeter in only twelve percent of all cases⁸, whereas this is twenty-four percent for conventional radiotherapy mask fixation⁹.

As a genuine image guided positioning system, ExacTrac teams up with Automatic Brain Metastases Planning to offer a frameless radiosurgery solution that allows unlimited intra-fraction positioning monitoring. ExacTrac is an essential complementary technology to both Novalis and Automatic Brain Metastases Planning.

The most important step in the image guided frameless radiosurgery workflow is the fusion of “live” localization images to digitally reconstructed radiographs or simulation images to determine the deviation from the desired patient position. The two minute reliable and fast fusion algorithm of ExacTrac has been reported to automatically achieve a correct fusion without manual correction in over 90% of all frameless radiosurgery cases¹⁰.

Table 2: Treatment Characteristics

Treatment Characteristics	Patient 1	Patient 2	Patient 3	Patient 4	Patient 5	Patient 6	Patient 7	Patient 8	Patient 9	Patient 10
Number of arcs	4	6	7	9	10	9	7	4	4	7
Number of couch angles	4	4	5	5	5	4	5	3	4	5
Average conformity index*	1.63	1.55	1.67	1.63	1.62	1.84	1.64	1.17	1.43	1.54
Number of monitor units	4,766	6,218	6,681	7,812	7,642	8,165	6,967	3,738	3,754	5,769
Total treatment planning time (min)	2	2	2	2	2	2	2	2	2	2
Beam-on time (min)	7.9	10.4	11.1	13.0	12.7	13.6	11.6	6.2	6.3	9.6

*Inverse Paddick Conformity Index

High quality imaging for localization and simulation is a necessity for reliable image fusion. For the localization images, ExacTrac accredits superior contrast resolution in optimal exposure conditions to the unique configuration of the X-Ray system. The fixed configuration of X-Ray tubes and flat-panel detectors eliminates any potential spatial uncertainty caused by mechanical movement. Furthermore, the large source-to-detector distance reduces the solid angle of the radiation beam and hence reduces potential geometric distortion. Finally, the large isocenter-to-detector distance reduces the potential body scattering to the detectors and hence increases the contrast to noise ratio¹¹.

With brain metastases typically scattered across the brain, the treatment isocenter is at a variable distance from each individual metastasis. This greatly impacts the effect of uncorrected translations and rotations with inaccuracies beyond two millimetres for metastases that are nine centimetres away from the isocenter¹². This could mean a complete miss for some of the smaller lesions from Table 1.

In order to enable true frameless radiosurgery and achieve sub-millimetre accuracy¹³, ExacTrac complements the standard couch with a robotic tilt module that fulfils corrections in pitch and roll. Because the isocenter is used as the rotational origin in the ExacTrac fusion algorithm, the rotations are decoupled from the translations and both sets of shifts can be safely and independently applied¹⁴.

All mechanical motion inherently produces additional inaccuracies and this paradigm also applies to movements of the treatment table. The need to detect and correct these errors together with possible patient motion inside the mask is obvious. Because ExacTrac is decoupled from the linear accelerator, it uniquely allows for X-Ray guided monitoring of the internal patient anatomy at all table angles. Moreover, ExacTrac offers the opportunity to correct detected shifts at any couch angle, making it perfectly suited for true frameless radiosurgery.

References

<p>[1] Sahgal A. et al., Int J Radiat Oncol 91, 710, 2015 [2] Bhatnagar A.K. et al., Int J Radiat Oncol Biol Phys 64, 898, 2006 [3] Minniti G. et al., Radiat Oncol 9, 110, 2014 [4] Inoue H. K. et al., Radiat Oncol 9, 231, 2014 [5] Fahrig A. et al., Strahlenther Onkol 183, 625, 2007 [6] Ernst-Stecken A. et al., Radiother Oncol 81, 18, 2006 [7] Torrens M. et al., J Neurosurg 121, 2, 2014</p>	<p>[8] Badakhshi H. et al., Cancer Radiothérapie 17, 664, 2013 [9] Lightstone A.W. et al., Technol Cancer Res Treat 11, 203, 2012 [10] Verellen D. et al., Radiother Oncol 67, 129, 2003 [11] Lee S.W. et al, J Appl Clin Med Phys 9(1), 1, 2008 [12] Tominaga H. et al., Phys Med Biol 59, 7753, 2014 [13] Gevaert T. et al., Int J Radiat Oncol 82, 1627, 2012 [14] Agazaryan N. et al., Phys Med Biol 53, 1715, 2008</p>
--	---